Neutron Diffraction Study on the Multiple Magnetization Plateaus in TbB_4 under Pulsed High Magnetic Field

S. Yoshii,[1] K. Ohoyama,[1] K. Kurosawa,[1] H. Nojiri,[1] M. Matsuda,[2] P. Frings,[2] F. Duc,[2] B. Vignolle,[2] G. L. J. A. Rikken,[3] L.-P. Regnault,[4] S. Michimura,[5] and F. Iga[5]

[1]*Institute for Materials Research, Tohoku University, Sendai 980-8577, Japan*
[2]*Quantum Beam Science Directorate, Japan Atomic Energy Agency–Tokai, Ibaraki 319-1195, Japan*
[3]*Laboratoire National des Champs Magnétiques Intenses, UPR3228 CNRS-INSA-UJF-UPS, Grenoble & Toulouse, France*
[4]*CEA-Grenoble, INAC-SPSMS-MDN, 17 rue des Martyrs, 38054 Grenoble Cedex 9, France*
[5]*ADSM, Hiroshima University, Higashi-Hiroshima 739-8530, Japan*

(Received 14 February 2009; published 12 August 2009)

We present the first application of pulsed high magnetic fields up to 30 T for neutron diffraction experiments. As the first study, field variations of a couple of magnetic Bragg reflections have successfully been measured in the frustrated antiferromagnet TbB_4. The results show that the conventional models fail, and a model, which is a mixture of the XY- and the Ising-type moments, matches for the half-magnetization state. We deduce an interaction that stabilizes an orthogonal moment arrangement as an origin of the unusual magnetization plateaus. Our results demonstrate the powerfulness of the present pulsed magnetic fields neutron diffraction system.

DOI: 10.1103/PhysRevLett.103.077203 PACS numbers: 75.25.+z, 75.30.Gw, 75.50.Ee

Magnetism of geometrically frustrated systems is among the hot topics in condensed matter physics. In such systems, a variety of unconventional phases appear due to a frustrated spin interaction that couples with lattice, orbital, and charge degrees of freedom. We can tune the balance between them using a strong magnetic field through the Zeeman interaction of spins, and various novel magnetic phases have been found in magnetic fields exceeding 20 T. Neutron scattering is a powerful and valuable technique to directly determine the space and time correlation of magnetic moments and to have a deeper insight into the origin of the novel phases in high fields. So far, however, sufficiently high magnetic fields have not been accessible for neutron scattering studies.

In this Letter, we present the first successful application of pulsed high magnetic fields for neutron diffraction experiments up to 30 T. This new technique was used to study the magnetic structure of the frustrated antiferromagnet TbB_4. The results give us a new element to understand the unusual multistep magnetization in TbB_4.

TbB_4 has a tetragonal structure ($P4/mbm$), in which the network of Tb ions in the ab plane is equivalent to the geometrically frustrated Shastry-Sutherland lattice (SSL) [1,2]. At $B = 0$ T, successive antiferromagnetic (AFM) transitions occur at $T_{N1} = 44$ K and $T_{N2} = 24$ K [3]. It has an XY-type noncollinear magnetic structure (see the inset in Fig. 1) [4]. The magnetic unit consists of four Tb moments in the crystal unit cell [i.e., a $\mathbf{k} = (0, 0, 0)$-type structure]. Between T_{N1} and T_{N2}, the moments point toward [110] and other equivalent directions, showing an orthogonal arrangement. Below T_{N2}, the moments [$8.2\mu_B$ at 3 K (μ_B is the Bohr magneton)] tilt about $\phi \sim 23°$ from the diagonal direction. Remarkably, below T_{N2}, multiple magnetization plateaus appear above 16 T at 2/9, 4/9, 1/2, and other fractions of the saturation magnetization M_s of $8.6\mu_B$/Tb, which is close to the free Tb^{3+} moment of $9\mu_B$, only when the magnetic field is perpendicular to the magnetic easy plane (Fig. 1) [1].

The dielectric $SrCu_2(BO_3)_2$ is a well studied implementation of the SSL system because magnetization plateaus appear in a two-dimensional (2D) spin gap system [5]. The plateaus in this quantum spin system are interpreted as the condensation of hopping triplets, which is analogous to Mott insulating (or charge density wave) phases, due to a repulsive interaction and limited hopping caused by strong frustration [6].

TbB_4, however, is a metal and a classical spin system. As found in CeSb [7], a stepwise magnetization in rare-earth intermetallics is usually expected along the Ising easy

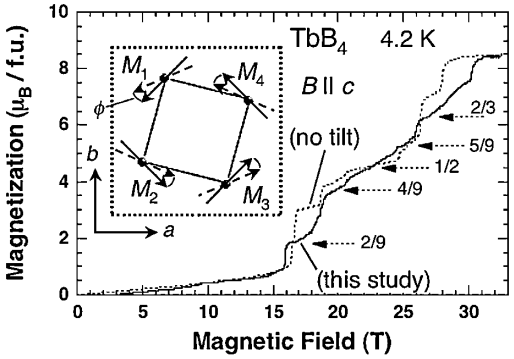

FIG. 1. Magnetization (M) of TbB_4 at 4.2 K (f.u. denotes formula unit). Dashed line: Magnetic field B is parallel to the c axis. Solid line: Field direction is tilted 5° from the c axis, which corresponds to this study. The indicated fraction denotes the ratio M/M_s. Inset: Magnetic structure at $B = 0$ T for $T_{N2} < T < T_{N1}$ (solid arrows) and $T < T_{N2}$ (dashed arrows) [4].

axis and is attributed to a competition of RKKY interactions with strong Ising anisotropy, as discussed in the axial next-nearest-neighbor Ising model or the incommensurate mean field model [8]. On the other hand, in TbB_4, it appears along the hard axis and cannot be explained by a model for the Ising system. Theoretically, the ground state of the classical SSL system is a helical antiferromagnet [2], and no metamagnetic transitions are expected in the direction perpendicular to the helical plane. In TbB_4, the orthogonal moment configuration below T_{N1} reminds us of a strong anisotropic interaction that competes with or dominates an isotropic AFM interaction. The series of unusual metamagnetic transitions in TbB_4 may originate from such anisotropic interaction. To clarify the interaction mechanism, a determination of magnetic structures at each plateau is essential.

The high field neutron diffraction experiment has been conducted with a combination of a newly developed pulsed magnet system and the reactor neutron source at the Institut Laue-Langevin (ILL) [Fig. 2(a)]. By using the continuous beam from a reactor, we can observe a continuous field variation of neutron intensity at a selected reflection point. A small magnet coil is mounted on a cryostat insert that can be mounted into the standard orange cryostat [9,10]. The 30 T pulsed field is generated by a transportable capacitor bank [11] every 5 minutes. The system is quite compact and can be easily installed at any neutron facility.

The experiment was performed on the high-flux, low-background triple-axis spectrometer IN22 at the ILL, with a neutron wavelength of 1.53 Å. A single crystal of TbB_4 enriched with ^{11}B ($4 \times 4 \times 3$ mm^3, 296 mg) was used. It was oriented with the field direction tilted 5° from the tetragonal c axis, owing to the asymmetric neutron path

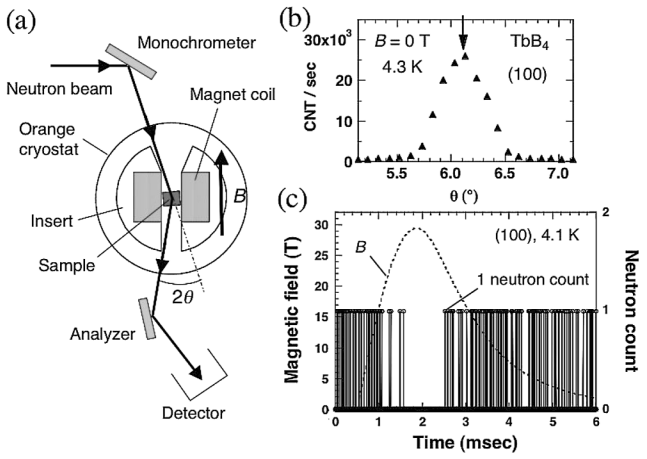

FIG. 2. (a) Schematic of the experimental setup. (b) (100) Bragg reflection profile at $B = 0$ T. During the high field experiment, θ was fixed at the peak position indicated by the arrow. (c) Time structures of the magnetic field (rising and falling time are 1.4 and 7 ms, respectively) and neutron count of a single magnetic pulse experiment. One vertical solid line corresponds to one neutron count.

inside the magnet coil. As shown in Fig. 1, this slight tilt does not destroy the stepwise aspect of the magnetization: The phase boundaries are mostly identical with those of the nontilted one. Four Bragg reflections [(100), (200), (110), and (220)] have been measured within the constraint of the accessible scattering angle θ ($2\theta = 30°$ at the center of the magnet coil) in the present system. The coil axis was set horizontally in the scattering plane. The sample was rearranged between the (h00) and the (hh0) experiments by rotating the sample holder about the coil axis. The θ was fixed at the peak position of each Bragg reflection at $B = 0$ T [see Fig. 2(b) for (100) reflection]. During the magnetic field pulse, the time structures of the field signal and neutron count were synchronously stored [Fig. 2(c)]. The time resolution of data taking is 0.8 μs, and the width of the neutron detector pulse is about 40 μs. These are sufficient due to the longer duration of the magnetic field. After time binning of the neutron count and correction of the neutron time of flight ($\approx$0.6 ms), the data were converted to a field dependence plot of the neutron count. The results shown here were taken by accumulating 100–200 magnetic field pulses for each reflection. The absence of a mechanical misalignment during the field pulse was confirmed by monitoring diffraction peaks that should not depend on the field. We also checked magnetostriction effects being negligible.

The $\mathbf{k} = (0, 0, 0)$ AFM structure at $B = 0$ T causes the appearance of the otherwise forbidden (100) reflection. The normalized values of the intensity I/I_0 and the magnetization M/M_s are presented in Fig. 3(a), at 4.1 K. [Hereafter, we use the normalized magnetic intensities in discussion. For (100), it is normalized to the zero field value I_0. For the other three reflections, the normalizations are made by the intensities I_s at the saturated ferromagnetic state.] As indicated by the dashed lines, stepwise changes of the intensity can be observed. The field region of each intensity plateau coincides with that of the magnetization plateau. The results show that an AFM component among 4 magnetic moments in the unit cell remains until the magnetization reaches the saturation. In this study, we mainly focus on the most important half-plateau phase ($21 \text{ T} < B < 24$ T) that is most robust. We have checked the peak profile of the (100) reflection in fields and confirmed that there is no obvious broadening or shift of the peak position, which may exclude a possible coexistence of two phases due to the tilting of the field direction at least in the $1/2M_s$ phase. We also note that the statistics becomes better at the plateau states in the higher field, since the time window is getting wider toward the field peak due to the smaller field variation in time. This enabled us to obtain reasonable data to discuss the half-plateau phase.

As a first approach, we consider two conventional magnetic structure models, an XY-type spin-flop structure (model A) and an Ising-type collinear one (model B), as

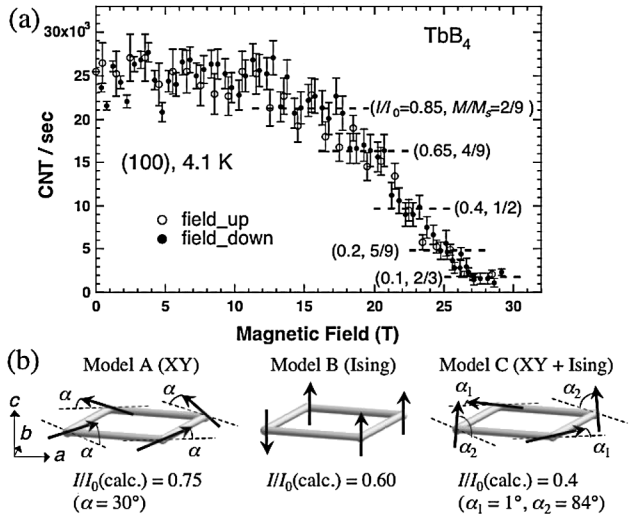

FIG. 3. (a) Field dependence of (100) reflection at 4.1 K for an ascending (open circles) and a descending (closed circles) field. The dashed lines represent the I/I_0 value at the center field of each plateau that is determined from the magnetization shown in Fig. 1. (b) Magnetic structure models for $M/M_s = 1/2$. Calculated I/I_0 of (100) reflection are presented. α, α_1, and α_2 are tilt angles toward the c axis from the ab plane.

shown in Fig. 3(b). (In our calculation, the magnitude of the Tb moment is assumed to be $9\mu_B$ for all of the considered structures.) Calculations of the magnetic structure factors clearly conclude that the XY model can explain none of the plateau states, and neither can a simple u-u-u-d collinear structure explain the $1/2M_s$ state: For example, the observed I/I_0 of about 0.4 for $M/M_s = 1/2$ is much smaller than the calculated values of 0.75 (XY model) and 0.6 (Ising model). Thus, the present experiment clearly confirms that the AFM correlation at high fields is weak as compared to what is expected for a conventional antiferromagnet. In contrast, model C in Fig. 3(b), which is a mixture of the planar-type and the Ising-type moments, is capable to explain the (100) intensity of the $1/2M_s$ state. Such an orthogonal arrangement again reminds us of a predominant anisotropic interaction in this system.

Magnetic reflection (200) originates from a total magnetization $\vec{M} = \vec{M}_1 + \vec{M}_2 + \vec{M}_3 + \vec{M}_4$ and is related to a ferromagnetic (FM) component. Both FM ($\vec{M}_1 + \vec{M}_3$ or/and $\vec{M}_2 + \vec{M}_4$) and AFM ($\vec{M}_1 - \vec{M}_3$) components, which come from a pair interaction along the [110] direction, produce magnetic scattering at (110) and (220). From magnetic structure factor consideration, reflection (110) is expected to be more sensitive to the appearance of a FM component than the (220) reflection. At $B = 0$ T, these three reflections contain only a nuclear scattering above T_{N2}. Below T_{N2}, a magnetic contribution superimposes in (110) and (220) reflections due to a nonzero ϕ, where the tilt induces an AFM ($\vec{M}_1 - \vec{M}_3$) component that is perpendicular to the scattering vector (see Fig. 1).

The field variations of (200), (110), and (220) reflections for $T < 4$ K are shown in Fig. 4(a). Remarkable is the absence of an enhancement of the (110) reflection in the $1/2M_s$ phase: In model C, the large FM ($\vec{M}_2 + \vec{M}_4$) component induces magnetic scattering, causing an enhancement of (110) reflection at the $1/2M_s$ phase, as shown in Fig. 4(c). This fact tells us that the 4 moments in the unit cell do not have a large c-axis component so that they produce less than one-half of the saturation magnetization. This means that the dominant FM component in the $1/2M_s$ phase is not described by the wave vector $\mathbf{k} = (0, 0, 0)$ and the magnetic unit cell is larger than the crystal unit cell.

As a preferable model for the $1/2M_s$ state, we propose a checkerboard structure formed by two types of square units [model D in Fig. 4(b)]. One unit consists of four planar-type moments, where the moments are almost confined in the ab plane but slightly tilted towards the c axis. In another unit, the moments stand up from the basal plane and are nearly parallel to the c axis. The calculated I/I_s of the (200), (110), and (220) reflections for model D are compared with those for model C in Fig. 4(c). Indeed, model D not only explains the (100) intensity quantitatively [I/I_0(calc.) ~ 0.38] but also qualitatively agrees with the other three reflections. In model D, the increases of the (200) and (220) intensities are attributed to a small c-axis component with $\mathbf{k} = (0, 0, 0)$ originating from the small canting of the 4 moments toward the c axis.

The SSL consists of square bonds (next-nearest-neighbor) and partial diagonal bonds (nearest-neighbor) [2]. The square system exhibits the orthogonal arrangement of moments in zero field as mentioned before. It is

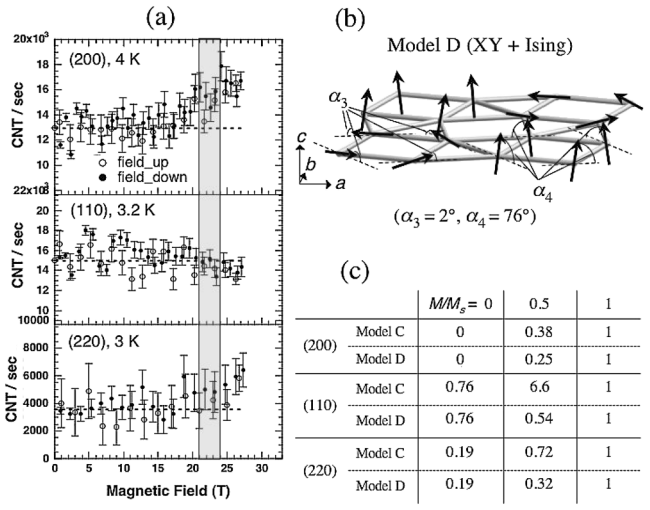

(c)

		M/M_s = 0	0.5	1
(200)	Model C	0	0.38	1
	Model D	0	0.25	1
(110)	Model C	0.76	6.6	1
	Model D	0.76	0.54	1
(220)	Model C	0.19	0.72	1
	Model D	0.19	0.32	1

FIG. 4. (a) Field variations of (200), (110), and (220) reflections for $T < 4$ K. The dashed lines represent the intensities at $B = 0$ T for each reflection. The field region for $M/M_s = 1/2$ state is shaded. (b) Magnetic structure model for $M/M_s = 1/2$ with a large magnetic unit cell. α_3 and α_4 are tilt angles toward the c axis from the ab plane. (c) Calculated magnetic intensity I/I_s for models C and D.

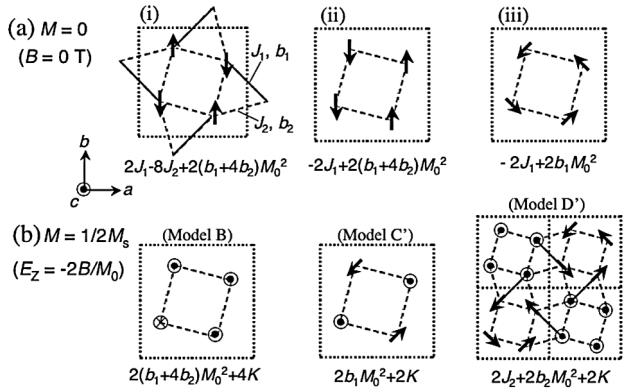

FIG. 5. Calculated energy E per unit cell for (a) $M = 0$ and (b) $M = 1/2M_s$ structures. The solid and dashed lines represent the nearest- and the next-nearest-neighbor interactions, respectively. Model C′ and model D′ are idealized versions of, respectively, model C and model D, in which $\phi = 0°$, $\alpha_1 = \alpha_3 = 0°$, and $\alpha_2 = \alpha_4 = 90°$.

worth noting that, in model D, all of the nearest-neighbor moments are nearly orthogonal. This encourages the idea that the diagonal interaction also prefers an orthogonal arrangement of moments in the field. From these, we may assume the presence of an interaction with a biquadratic form $b_i(\vec{M}_j \cdot \vec{M}_k)^2$, which stabilizes moments being perpendicular to each other for $b_i > 0$. Here we briefly discuss the magnetic structure based on the SSL model including this biquadratic interaction. The free energy is given by $E = E_{\mathrm{exch}} + E_{\mathrm{bq}} + E_a + E_Z$. The E_{exch} represents the bilinear interaction $J_i\vec{M}_j \cdot \vec{M}_k$. The E_{bq} is the biquadratic interaction. (J_1, b_1) and (J_2, b_2) correspond to the interactions on the diagonal and square bonds, respectively. The last two terms are an anisotropy energy $E_a = M_0^2 \sum_i K \sin^2\beta_i$ $(K > 0)$ and the Zeeman term E_Z, where β_i is the angle from the ab plane and M_0 is the magnitude of moment $\vec{M}_j$. The calculated energies E per unit cell are compared for several structures with $M = 0$ [Fig. 5(a)] and $M = 1/2M_s$ [Fig. 5(b)]. In the ground state, the antiparallel moments on the diagonal bonds become stable for $J_1 > 2J_2$ [see Figs. 5(a)(i) and 5(a)(ii)]. Then the perpendicular structure [Fig. 5(a)(iii)] gains energy with respect to the collinear one [Fig. 5(a)(ii)], if $b_2 > 0$. Regarding the $1/2M_s$ structure, model C′ has the same E_{bq} as that of Fig. 5(a)(iii). When the b_1 interaction is dominant and satisfies the relation $J_2 + b_2M_0^2 < b_1M_0^2$, model D′ becomes stable against model C′.

These considerations stimulate a qualitative scenario for the appearance of magnetization plateaus in TbB_4. In the SSL, magnetic frustration occurs when the AFM interactions J_1 and J_2 are comparable. In the same sense, the biquadratic interaction is frustrated for a special ratio of b_1 and b_2, and the E_{bq} of several structures must be close to each other. At zero field, the magnetic moments lie in the ab plane due to the easy-plane anisotropy. As an excited state, several states are degenerate in energy E_{bq}, where some of the moments have an orthogonal arrangement due to the large b_1 interaction. When a gain of the E_Z compensates the cost in the E_a, one of the degenerate states must be stabilized in a certain field region, which produces a stepwise change of magnetization. Such a process may occur step by step with increasing field, owing to a delicate balance among bilinear interactions, biquadratic interactions, and easy-plane anisotropy. As for the origin of b, a quadrupole interaction may be possible, as commonly discussed for rare-earth compounds [12]. A theoretical study, taking these interactions into account, is desired to fully understand the complex magnetization process, which is beyond the scope of this work.

In summary, our results confirm that the conventional model fails in TbB_4 and indicate the predominant anisotropic interaction. We propose a checkerboard model for the $1/2M_s$ state that matches with the experiment. We suggest the biquadratic interaction b as a possible mechanism for the magnetization plateaus, where the b stabilizes an orthogonal moment arrangement.

As demonstrated, our new technique is a powerful tool to investigate field-induced phases under high magnetic fields. This will open the door for new investigations in a wide variety of systems, such as the frustrated magnets, strongly correlated electron systems, and so on.

This work was supported by a Grant-in-Aid for Scientific Research on priority Areas High Field Spin Science in 100 T (No. 451) and Fundamental Research C (No. 16540319) from the Ministry of Education, Culture, Sports, Science and Technology of Japan and the Agence National de la Recherche (No. NT05-4-42463).

[1] S. Yoshii *et al.*, Phys. Rev. Lett. **101**, 087202 (2008).
[2] B. S. Shastry and B. Sutherland, Physica (Amsterdam) **108B+C**, 1069 (1981).
[3] Z. Fisk *et al.*, Solid State Commun. **39**, 1189 (1981).
[4] T. Matsumura *et al.*, J. Phys. Soc. Jpn. **76**, 015001 (2007).
[5] H. Kageyama *et al.*, Phys. Rev. Lett. **82**, 3168 (1999).
[6] See, for example, S. Miyahara and K. Ueda, J. Phys. Condens. Matter **15**, R327 (2003).
[7] J. Rossat-Mignot *et al.*, J. Magn. Magn. Mater. **31–34**, 398 (1983).
[8] M. Date, J. Phys. Soc. Jpn. **57**, 3682 (1988).
[9] K. Ohoyama *et al.*, J. Phys. Conf. Ser. **51**, 506 (2006).
[10] K. Ohoyama *et al.*, J. Magn. Magn. Mater. **310**, e974 (2007).
[11] P. Frings *et al.*, Rev. Sci. Instrum. **77**, 063903 (2006).
[12] P. Morin and D. Schmitt, in *Ferromagnetic Materials*, edited by K. H. J. Bushow and E. P. Wohlfarth (Elsevier Science, Amsterdam, 1990), Vol. 5, p. 1.